

# The effect of cobalt doping on the morphology and electrochemical performance of high-voltage spinel $\text{LiNi}_{0.5}\text{Mn}_{1.5}\text{O}_4$ cathode material

Jing Mao<sup>a,b,c</sup>, Mengze Ma<sup>a,b</sup>, Panpan Liu<sup>a,b</sup>, Junhua Hu<sup>a,b</sup>, Guosheng Shao<sup>a,b</sup>, Vince Battaglia<sup>c</sup>, Kehua Dai<sup>d,c,\*</sup>, Gao Liu<sup>c,\*\*</sup>

<sup>a</sup> School of Materials Science and Engineering, Zhengzhou University, Zhengzhou 450002, China

<sup>b</sup> International Joint Research Laboratory for Low-Carbon & Environmental Materials of Henan Province, Zhengzhou University, Zhengzhou 450002, China

<sup>c</sup> Energy Storage and Distributed Resource Division, Energy Technologies Area, Lawrence Berkeley National Laboratory, Berkeley, CA 94720, USA

<sup>d</sup> School of Materials and Metallurgy, Northeastern University, Shenyang 110004, China

## ARTICLE INFO

### Article history:

Received 12 October 2015

Received in revised form 17 May 2016

Accepted 18 May 2016

Available online 3 June 2016

### Keywords:

High-voltage spinel

Lithium nickel manganese oxide

Lithium chemical diffusion coefficient

Cycling performance

Rate performance

## ABSTRACT

To reveal the effects of Co-doping on the electrochemical performance of micro-sized  $\text{LiNi}_{0.5}\text{Mn}_{1.5}\text{O}_4$  (LNMO), undoped LNMO and Co-doped  $\text{LiCo}_{0.1}\text{Ni}_{0.45}\text{Mn}_{1.45}\text{O}_4$  (LCoNMO) are synthesized via a PVP-combustion method and calcined at 1000 °C for 6 h. SEM and XRD analyses suggest that Co-doping decreases the particle size and the  $\text{Li}_2\text{Ni}_{1-z}\text{O}_2$  impurity at the calcination temperature of 1000 °C. LCoNMO has much better rate capability while its specific capacity at C/5 is 10% lower than that of LNMO. At 15 C rate, their specific capacities are closed, and the LCoNMO delivers 86.2% capacity relative to C/5, and this value for LNMO is only 77.0%. The  $D_{\text{Li}^+}$  values determined by potential intermittent titration technique (PITT) test of LCoNMO are 1–2 times higher than that of LNMO in most SOC region. The LCoNMO shows very excellent cycling performance, which is the best value compared with literatures. After 1000 cycles, the LCoNMO still delivers 94.1% capacity. Moreover, its coulombic efficiency and energy efficiency keep at 99.84% and over 97.3% during 1 C cycling, respectively.

© 2015 Published by Elsevier B.V.

## 1. Introduction

Next generation lithium-ion batteries for EV, HEV, energy storage, etc. request high energy density, high operation voltage, high rate capability and cycling stability cathode materials.  $\text{LiMn}_{1.5}\text{Ni}_{0.5}\text{O}_4$  (LNMO) with spinel structure is a promising candidate for its high working voltage of ~4.7 V and capacity of ~130 mAh g<sup>-1</sup> [1–7]. The main concern about this material is the capacity fading in full cells due to electrolyte decomposition and concurrent degradative reactions at electrode/electrolyte interfaces [5,8–10]. Moreover, comparing to spinel  $\text{LiMn}_2\text{O}_4$ , LNMO shows lower rate performance and needs to be improved by doping.

Doping is one of the most popular ways to improve the cycling performance and/or rate performance of LNMO [11,12]. Among the reported doping cations and anions [11,13–34], Co-doping shows great improvement on rate capability and cycling stability of LNMO [2,6,19,21,28]. We previously reported micro-sized LNMO synthesized via a PVP-combustion method with excellent rate capability and cycling stability [35]. Thus, further improvement of rate and cycling performance

could be anticipated by combining Co-doping and PVP-combustion method.

In this paper, undoped  $\text{LiNi}_{0.5}\text{Mn}_{1.5}\text{O}_4$  (LNMO) and Co-doped  $\text{LiCo}_{0.1}\text{Ni}_{0.45}\text{Mn}_{1.45}\text{O}_4$  (LCoNMO) are synthesized via PVP-combustion method and calcined at 1000 °C for 6 h. The improved rate capability and the very excellent cycling stability of LCoNMO are exhibited.

## 2. Experimental

### 2.1. Synthesis procedure

The undoped  $\text{LiNi}_{0.5}\text{Mn}_{1.5}\text{O}_4$  (LNMO) and Co-doped  $\text{LiCo}_{0.1}\text{Ni}_{0.45}\text{Mn}_{1.45}\text{O}_4$  (LCoNMO) were prepared by polyvinylpyrrolidone (PVP)-combustion method. In detail, stoichiometric  $\text{LiOAc} \cdot 2\text{H}_2\text{O}$ ,  $\text{Ni}(\text{NO}_3)_2 \cdot 6\text{H}_2\text{O}$ ,  $\text{Mn}(\text{OAc})_2 \cdot 4\text{H}_2\text{O}$ ,  $\text{Co}(\text{OAc})_2 \cdot 4\text{H}_2\text{O}$ , and PVP (the molar ratio of PVP monomer to total metal ions was 2:1) were dissolved in deionized water and pH = 3 was achieved by adding 1:1  $\text{HNO}_3$ . The mixture was stirred at 120 °C to obtain a dry gel, which was ignited on a hot plate to induce a combustion process that lasted for several minutes. The resulting precursor was preheated at 450 °C for 3 h and then calcined at 1000 °C for 6 h with the heating rate of 5 °C min<sup>-1</sup>. After the heating treatment, the oven was switched off and the sample was cooled down naturally.

\* Correspondence to: K. Dai, School of Materials and Metallurgy, Northeastern University, Shenyang 110004, China.

\*\* Corresponding author.

E-mail addresses: [daikh@smm.neu.edu.cn](mailto:daikh@smm.neu.edu.cn) (K. Dai), [gliu@lbl.gov](mailto:gliu@lbl.gov) (G. Liu).

## 2.2. Morphology and structure characterization

The analysis of the phase purity and the structural characterization were made by X-ray powder diffraction (XRD) using a Bruker D2 PHASER diffractometer equipped with Cu K $\alpha$  radiation that was operated over a  $2\theta$  range of  $10\text{--}70^\circ$  in a continuous scan mode with a step size of  $0.004^\circ$ . The morphology was examined using a JEOL 7500F scanning electron microscope (SEM).

## 2.3. Electrochemical tests

The cathode was prepared by mixing 82 wt.% active material, 10 wt.% acetylene black (AB) and 8 wt.% polyvinylidene fluoride (PVDF) binder in N-methylpyrrolidone (NMP) to form a slurry. The slurry was doctor-bladed onto an aluminum foil, dried at  $60^\circ\text{C}$ , and then punched into electrode disks with a diameter of 12.7 mm. The prepared electrodes were dried at  $130^\circ\text{C}$  for 12 h in a vacuum oven and show typically an active material loading of about 5 mg. The electrochemical cells were fabricated with the LNMO cathode, lithium foil anode,  $1\text{ mol L}^{-1}$  LiPF $_6$  in 1:1 EC/DEC as electrolyte, and Celgard 2400 as separator in an argon-filled glove box. Electrochemical performances were evaluated using CR2325 coin cells. Galvanostatic charge–discharge tests were performed using Maccor 4000. The potential intermittent titration technique (PITT) test was conducted using a Bio-Logic VMP-3 multichannel electrochemical analyzer.

## 3. Results and discussion

Fig. 1 shows the SEM images of LNMO and LCoNMO. The shapes of particles for LNMO and LCoNMO have not much difference while small and big particles are less for LCoNMO. The particle size distributions are counted from 200 particles in lower magnification SEM images and are shown in Fig. 2 and Table 1. It can be seen that the mean particle size becomes smaller and the particles whose sizes are between 4 and  $5\ \mu\text{m}$  are less with Co-doping. The more centralized particle size distribution and smaller standard deviation value for LCoNMO indicate more uniform particle sizes.

Fig. 3 shows the XRD patterns of LNMO and LCoNMO. All diffraction peaks can be indexed as a cubic spinel structure and  $Fd\bar{3}m$  space group, and all of the peaks are narrow and sharp, indicating good crystallinity. The pattern of LNMO shows a weak peak related to  $\text{Li}_2\text{Ni}_{1-z}\text{O}_2$  at  $2\theta \approx 43.7^\circ$  [20] while this peak for LCoNMO is much weaker. The suppression of  $\text{Li}_2\text{Ni}_{1-z}\text{O}_2$  in high-voltage LNMO by Co-doping agrees with previous report [28].

Fig. 4a displays the charge and discharge profiles of LNMO and LCoNMO at C/5 rate in the 5th cycle. The charge capacity of LNMO and LCoNMO are  $136.4$  and  $120.8\text{ mAh g}^{-1}$ , respectively, and the discharge

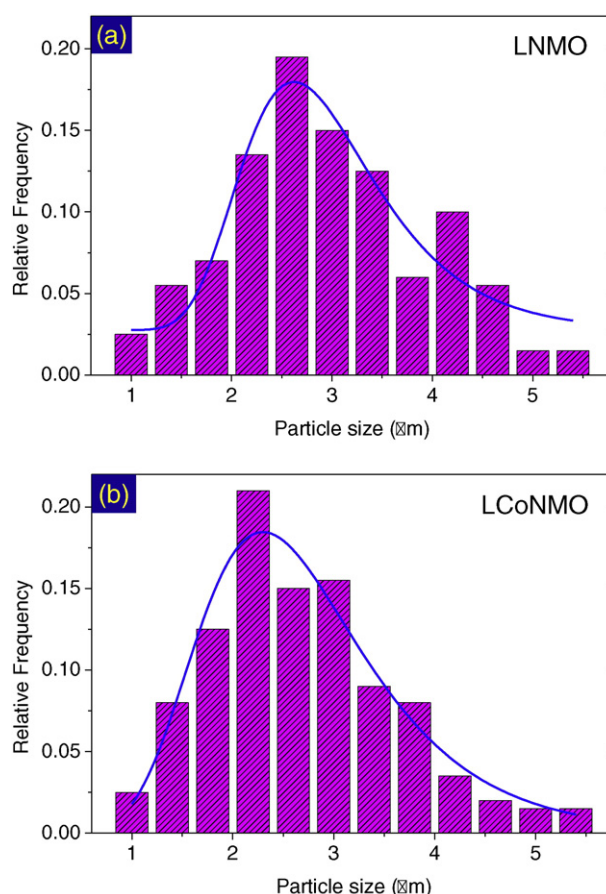


Fig. 2. The Particle size distributions of LNMO and LCoNMO.

capacity of LNMO and LCoNMO are  $130.3$  and  $117.3\text{ mAh g}^{-1}$ , respectively. The 10% capacity loss for the LCoNMO is due to the 10% decrease of Ni content relative to the LNMO and the  $\text{Co}^{3+}/\text{Co}^{4+}$  redox is not active below 5 V in this material [36,37]. The coulombic efficiency of LNMO and LCoNMO are 95.5% and 97.1% respectively. The higher coulombic efficiency for LCoNMO indicates less side reactions. The charge and discharge profiles of LNMO and LCoNMO both show three plateaus which suggest  $Fd\bar{3}m$  space group [38–41]. It is well known that the 4.6 V and 4.7 V plateaus are related to  $\text{Ni}^{2+}/\text{Ni}^{3+}$  and  $\text{Ni}^{3+}/\text{Ni}^{4+}$  redox, and the 4.0 V plateau is caused by  $\text{Mn}^{3+}/\text{Mn}^{4+}$  [27]. The 4.7 V plateau is higher and the 4.6 V plateau is lower for the LCoNMO than that for the LNMO. The voltage of the 4.7 V peaks in the  $dQ/dV$  curves (Fig. 4b) for

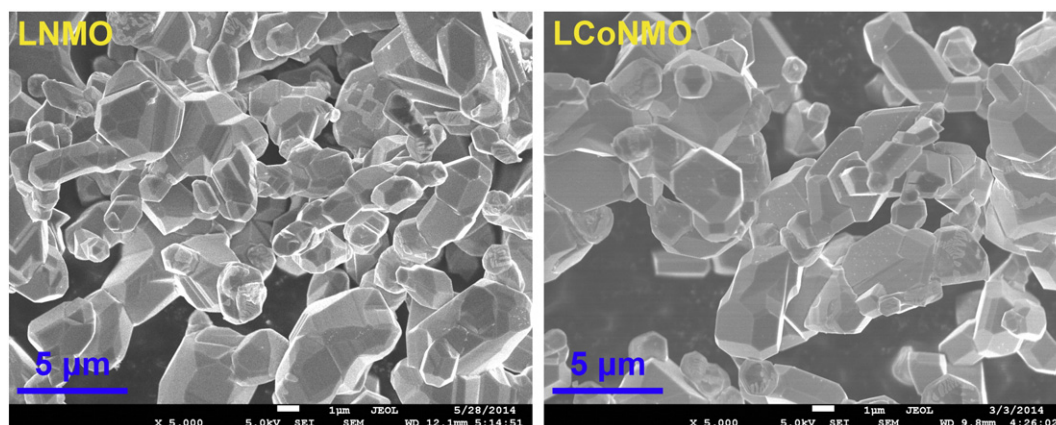


Fig. 1. The SEM images of LNMO and LCoNMO.

Download English Version:

<https://daneshyari.com/en/article/1296055>

Download Persian Version:

<https://daneshyari.com/article/1296055>

[Daneshyari.com](https://daneshyari.com)